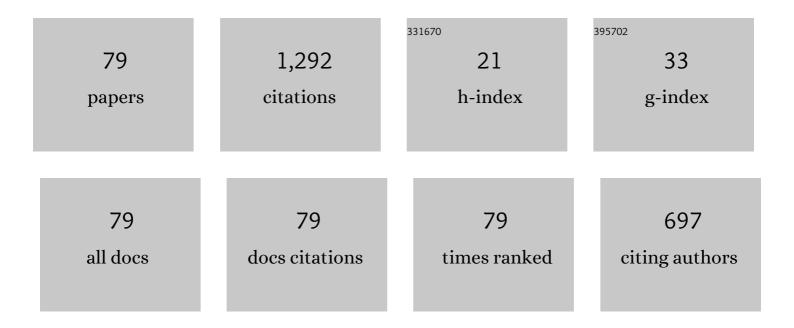
Xiong Wang

List of Publications by Year in descending order

Source: https://exaly.com/author-pdf/2009178/publications.pdf Version: 2024-02-01



XIONC WANC

#	Article	IF	CITATIONS
1	3-D Manipulation of Dual-Helical Electromagnetic Wavefronts With a Noninterleaved Metasurface. IEEE Transactions on Antennas and Propagation, 2022, 70, 378-388.	5.1	26
2	Microwave-Induced Thermoacoustic Imaging of Small Animals Applying Scanning Orthogonal Polarization Excitation. IEEE Journal of Electromagnetics, RF and Microwaves in Medicine and Biology, 2022, 6, 123-130.	3.4	8
3	Multiple Back Projection With Impact Factor Algorithm Based on Circular Scanning for Microwave-Induced Thermoacoustic Tomography. IEEE Journal of Electromagnetics, RF and Microwaves in Medicine and Biology, 2022, 6, 182-188.	3.4	1
4	Enhanced Subâ€Terahertz Microscopy based on Broadband Airy Beam. Advanced Materials Technologies, 2022, 7, 2100985.	5.8	13
5	Shaping Electromagnetic Fields with Irregular Metasurface. Advanced Materials Technologies, 2022, 7,	5.8	12
6	Balanced-ternary-inspired reconfigurable vortex beams using cascaded metasurfaces. Nanophotonics, 2022, 11, 2369-2379.	6.0	14
7	Single-Layer Noninterleaved Metasurface for Arbitrary Vector Beam Conversion in Triple Bands. ACS Applied Electronic Materials, 2022, 4, 443-451.	4.3	3
8	Fourâ€Channel Kaleidoscopic Metasurfaces Enabled by a Singleâ€Layered Singleâ€Cell Quadâ€Band Metaâ€Aton Advanced Theory and Simulations, 2022, 5, .	^{1.} 2.8	4
9	Highâ€Efficiency Fullâ€Space Complexâ€Amplitude Metasurfaces Enabled by a Biâ€Spectral Singleâ€Substrateâ€ Metaâ€Atom. Advanced Optical Materials, 2022, 10, .	Layer 7.3	15
10	Cryptography Metasurface for Oneâ€Timeâ€Pad Encryption and Massive Data Storage. Laser and Photonics Reviews, 2022, 16, .	8.7	14
11	Characterization of Orbital Angular Momentum Applying Single-Sensor Compressive Imaging Based on a Microwave Spatial Wave Modulator. IEEE Transactions on Antennas and Propagation, 2021, 69, 6870-6880.	5.1	13
12	TM-polarized angle-dispersive metasurface for axisymmetric extension of beam steering angles. Optics Express, 2021, 29, 3211.	3.4	3
13	Single-layered meta-reflectarray for polarization retention and spin-encrypted phase-encoding. Optics Express, 2021, 29, 3230.	3.4	27
14	A Preclinical System Prototype for Focused Microwave Breast Hyperthermia Guided by Compressive Thermoacoustic Tomography. IEEE Transactions on Biomedical Engineering, 2021, 68, 2289-2300.	4.2	37
15	A Low-Cost Compressive Thermoacoustic Tomography System for Hot and Cold Foreign Bodies Detection. IEEE Sensors Journal, 2021, 21, 23588-23596.	4.7	15
16	2-D Noninvasive Temperature Measurement of Biological Samples Based on Compressive Thermoacoustic Tomography. IEEE Journal of Electromagnetics, RF and Microwaves in Medicine and Biology, 2021, 5, 371-378.	3.4	10
17	Correction to "Focused Microwave Breast Hyperthermia Monitored by Thermoacoustic Imaging: A Computational Feasibility Study Applying Realistic Breast Phantoms―[Jun 20 81-88]. IEEE Journal of Electromagnetics, RF and Microwaves in Medicine and Biology, 2021, 5, 194-194.	3.4	0
18	Ultrabroadband microwave absorber based on 3D water microchannels. Photonics Research, 2021, 9, 1391.	7.0	27

#	Article	IF	CITATIONS
19	Multichannel Highâ€Efficiency Metasurfaces Based on Triâ€Band Singleâ€Cell Metaâ€Atoms with Independent Complexâ€Amplitude Modulations. Advanced Photonics Research, 2021, 2, 2100088.	3.6	6
20	Polarizationâ€Assisted Visual Secret Sharing Encryption in Metasurface Hologram. Advanced Photonics Research, 2021, 2, 2100175.	3.6	11
21	Three-Dimensional Microwave-Induced Thermoacoustic Imaging Based on Compressive Sensing Using an Analytically Constructed Dictionary. IEEE Transactions on Microwave Theory and Techniques, 2020, 68, 377-386.	4.6	34
22	Focused Microwave Breast Hyperthermia Monitored by Thermoacoustic Imaging: A Computational Feasibility Study Applying Realistic Breast Phantoms. IEEE Journal of Electromagnetics, RF and Microwaves in Medicine and Biology, 2020, 4, 81-88.	3.4	37
23	Frequencyâ€Multiplexed Complexâ€Amplitude Metaâ€Devices Based on Bispectral 2â€Bit Coding Metaâ€Atoms. Advanced Optical Materials, 2020, 8, 2000919.	7.3	27
24	Fast Thermoacoustic Imaging Based on Compressive Sensing Applying an Effective Algorithm. , 2020, , .		1
25	Multifunctional Geometric Metasurfaces Based on Triâ€Spectral Metaâ€Atoms with Completely Independent Phase Modulations at Three Wavelengths. Advanced Theory and Simulations, 2020, 3, 2000099.	2.8	13
26	Angle-Dispersive Metasurface for Axisymmetric Wavefront Manipulation over Continuous Incident Angles. Physical Review Applied, 2020, 14, .	3.8	5
27	Broadband High-Efficiency Electromagnetic Orbital Angular Momentum Beam Generation Based on a Dielectric Metasurface. IEEE Photonics Journal, 2020, 12, 1-11.	2.0	20
28	3-D Printed Swastika-Shaped Ultrabroadband Water-Based Microwave Absorber. IEEE Antennas and Wireless Propagation Letters, 2020, 19, 821-825.	4.0	53
29	Full control of dual-band vortex beams using a high-efficiency single-layer bi-spectral 2-bit coding metasurface. Optics Express, 2020, 28, 17374.	3.4	42
30	Broadband high-efficiency multiple vortex beams generated by an interleaved geometric-phase multifunctional metasurface. Optical Materials Express, 2020, 10, 1531.	3.0	29
31	Investigation on Distribution of Measurements for Microwave-induced Thermoacoustic Imaging Based on Compressive Sensing. , 2020, , .		2
32	Broadband high-efficiency multiple vortex beams generated by an interleaved geometric-phase multifunctional metasurface. Optical Materials Express, 2020, 10, 1531.	3.0	8
33	Reconfigurable metamaterial for chirality switching and selective intensity modulation. Optics Express, 2020, 28, 34804.	3.4	9
34	A Computational Study on Number of Elements in Antenna Array for Focused Microwave Breast Hyperthermia. , 2019, , .		6
35	Physical Mechanism and Response Characteristics of Unsaturated Optical Stopping-Based Amorphous Arsenic Sulfide Thin-Film Waveguides. IEEE Photonics Journal, 2019, 11, 1-10.	2.0	13
36	Highâ€Efficiency Ultrathin Dualâ€Wavelength Pancharatnam–Berry Metasurfaces with Complete Independent Phase Control. Advanced Optical Materials, 2019, 7, 1900594.	7.3	67

#	Article	IF	CITATIONS
37	Thermoacoustic Imaging Based on Sparse Measurements: A Computational Study Using Closely Located Samples. , 2019, , .		0
38	A Preliminary Study of Applying Microwave-induced Thermoacoustic Imaging to Detect Cold Targets. , 2019, , .		1
39	Enhanced and modulated microwave-induced thermoacoustic imaging by ferromagnetic resonance. Applied Physics Express, 2019, 12, 077001.	2.4	19
40	Microwave-Induced Thermoacoustic Imaging for Embedded Explosives Detection in High-Water Content Medium. IEEE Transactions on Antennas and Propagation, 2019, 67, 4803-4810.	5.1	25
41	Time-efficient Thermoacoustic Imaging with High Resolution for A Large Sample: A Simulation Study. , 2019, , .		Ο
42	Investigation on Effects of Acoustic Heterogeneity in Thermoacoustic Imaging Based on Compressive Sensing: A Simulation Study. , 2019, , .		0
43	Detecting Microwave Orbital Angular Momentum by Single-sensor Imaging: A Computational Feasibility Study. , 2019, , .		Ο
44	Investigation on Resolution of Thermoacoustic Imaging Based on Compressive Sensing: A Simulation Study. , 2019, , .		0
45	Improved Reconstruction Method Based on k-Means by Finding Peak Density Automatically in Microwave Induced Thermoacoustic Tomography. , 2019, , .		1
46	Generation of Broadband Quasi-Bessel Beams in Sub-THz Regime and Applications in Imaging. , 2019, , .		0
47	Generation of Tilted High-Order Bessel Beam in Millimeter Range Using Metasurface. , 2019, , .		1
48	Contrast-enhanced Thermoacoustic Imaging for Breast Tumor Detection with Sparse Measurements. , 2018, , .		0
49	Design of Thermoacoustic Monitoring System for Hyperthermia. , 2018, , .		6
50	Comparison of Two Optimization Algorithms for Focused Microwave Breast Cancer Hyperthermia. , 2018, , .		4
51	Metasurface for Generating High-Order Millimeter Wave Orbital Angular Momentum Beams. , 2018, , .		5
52	Metasurface-based broadband orbital angular momentum generator in millimeter wave region. Optics Express, 2018, 26, 25693.	3.4	84
53	A Novel Microwave Power Deposition Monitoring Method by Thermoacoustic Imaging (invited paper). , 2018, , .		0
54	Contribution assessment of antenna structure and in-gap photocurrent in terahertz radiation of photoconductive antenna. Journal of Applied Physics, 2018, 124, 053107.	2.5	7

#	Article	IF	CITATIONS
55	Feasibility Study of Applying Ferromagnetic Contrast Agents in Thermoacoustic Imaging. , 2018, , .		1
56	3D thermoacoustic imaging based on compressive sensing. , 2018, , .		4
57	A novel monitoring technique for breast cancer hyperthermia using thermoacoustic imaging. , 2018, , .		7
58	Microwave-Induced Thermoacoustic Communications. IEEE Transactions on Microwave Theory and Techniques, 2017, 65, 3369-3378.	4.6	40
59	Moving toward optoelectronic logic circuits for visible light: a chalcogenide glass single-mode single-polarization optical waveguide switch. Applied Optics, 2017, 56, 1405.	2.1	8
60	Thermoacoustic and photoacoustic characterizations of few-layer graphene by pulsed excitations. Applied Physics Letters, 2016, 108, .	3.3	36
61	Fabrication of a realistic breast phantom based on 3D printing technology for thermoacoustic imaging application in breast cancer detection. , 2015, , .		2
62	Broadband Spectroscopic Thermoacoustic Characterization of Single-Walled Carbon Nanotubes. Journal of Spectroscopy, 2015, 2015, 1-7.	1.3	8
63	Modeling of non-contact thermoacoustic imaging. , 2015, , .		4
64	Emergence of a virulent porcine reproductive and respiratory syndrome virus in vaccinated herds in the United States. Virus Research, 2015, 210, 34-41.	2.2	47
65	Computational Feasibility Study of Contrast-Enhanced Thermoacoustic Imaging for Breast Cancer Detection Using Realistic Numerical Breast Phantoms. IEEE Transactions on Microwave Theory and Techniques, 2015, 63, 1489-1501.	4.6	62
66	Quality Improvement of Thermoacoustic Imaging Based on Compressive Sensing. IEEE Antennas and Wireless Propagation Letters, 2015, 14, 1200-1203.	4.0	31
67	Numerical analysis of terahertz generation characteristics of photoconductive antenna. , 2014, , .		4
68	Non-contact thermoacoustic imaging based on laser and microwave vibrometry. , 2014, , .		7
69	Comparison of carbon nanotubes and microbubbles as contrast agents for thermoacoustic imaging by computational studies. , 2014, , .		3
70	Time-efficient contrast-enhanced thermoacoustic imaging modality for 3-D breast cancer detection using compressive sensing. , 2014, , .		12
71	Microwave-induced thermoacoustic imaging for embedded explosives detection. , 2014, , .		2
72	Microwave (1.7–2.6 GHz) characterization of hydroxylapatite and oxalate using rectangular waveguide. , 2014, , .		0

#	Article	IF	CITATIONS
73	A hybrid microwave / acoustic communication scheme — Thermoacoustic communication. , 2013, , .		6
74	Computational study of thermoacoustic imaging for breast cancer detection using a realistic breast model. , 2013, , .		4
75	Microwave-Induced Thermoacoustic Imaging Model for Potential Breast Cancer Detection. IEEE Transactions on Biomedical Engineering, 2012, 59, 2782-2791.	4.2	126
76	Impact of Microwave Pulses on Thermoacoustic Imaging Applications. IEEE Antennas and Wireless Propagation Letters, 2012, 11, 1634-1637.	4.0	36
77	Spectroscopic thermoacoustic imaging of water and fat composition. Applied Physics Letters, 2012, 101, .	3.3	55
78	Microwave induced thermal acoustic imaging modeling for potential breast cancer detection. , 2011, , .		3
79	Thermoacoustic imaging and spectroscopy for enhanced breast cancer detection. , 2011, , .		6